J|A|C|S
ARTICLES
Published on Web 07/19/2002

Flexible Sorption and Transformation Behavior in a Microporous Metal-Organic Framework

Edmund J. Cussen,[†] John B. Claridge,[†] Matthew J. Rosseinsky,*[,†] and Cameron J. Kepert[‡]

Contribution from the Department of Chemistry, University of Liverpool, Liverpool, U.K. L69 7ZD, and School of Chemistry, Heavy Metals Centre, University of Sydney, NSW 2006, Australia

Received March 21, 2002

Abstract: Crystals of the metal-organic framework material $Ni_2(4,4'\text{-bipyridine})_3(NO_3)_4$ (**A**) have been grown by reaction of $Ni(NO_3)_2{\cdot}6H_2O$ and 4,4′-bipyridine in methanol solution. Single-crystal X-ray diffraction experiments show that the ladder structure of the framework is maintained after desolvation of the material, resulting in the production of a porous solid stable to 215(4) °C. Powder X-ray diffraction has been employed to confirm the bulk purity and temperature stability of this material. The crystal structure indicates that the pore window has an area of 12.3 Å^2. However, sorption experiments show these windows will admit toluene, which has a minimum cross-sectional area of 26.6 Å^2, with no significant change in the structure. Monte Carlo docking calculations show that toluene can be accommodated within the large pores of the structure. Exposure of the related microporous material $Ni_2(4,4'\text{-bipyridine})_3(NO_3)_4{\cdot}2C_2H_5OH$ (**B**) to methanol vapor causes a guest-driven solid-state transformation to **A** which is observed using powder X-ray diffraction. This structural rearrangement proceeds directly from crystalline **B** to crystalline **A** and is complete in less than 1 day. Mechanisms for the transformation are proposed which require breaking of at least one in six of the covalent bonds that confer rigidity on the framework.

Introduction

The class of materials known as coordination polymers (or metal-organic frameworks) continues to be a growing area of interest[1−5] since research in the field was initiated a decade ago.[6] During this time, the state-of-the-art has advanced from the construction of frameworks of topological interest,[7] but low structural stability, to materials which show unprecedented pore volumes for a crystalline material.[8] The development of porosity has led to discussion of these materials finding application in areas such as gas separation,[9] guest storage,[10] and catalysis where microporous materials, for example, zeolites,[11] have traditionally found application. The wide range of network topologies and chemical functionalities which can be built into the framework has also aroused interest due to the possibility of preparing porous chiral materials. Chirality can arise from the use of an enantiomeric molecule in the construction of the framework[4] or from the assembly of achiral materials into a chiral framework,[12] and such materials offer promise in developing porous materials for enantiomeric separation, an application for which no suitable zeolite exists.

The metal-organic framework field has thus far been driven forward largely by new materials discovery, with less emphasis on detailed comparison of properties with previous, well-established classes of porous solids. Understanding of this sort will be essential in permitting any detailed application of this class of compound. The development of metal-organic framework materials for these applications will require a thorough understanding of the porosity within these materials in view of the substantial energy difference between the coordinate bonds sustaining these frameworks and the very strong Si/Al−O bonds in zeolites. On the basis of single-crystal structure determinations which demonstrate that the framework shows only a small distortion in response to guest loss,[13,14] and the observation of type I adsorption isotherms,[15] the porosity in these materials

* To whom correspondence should be addressed. E-mail: m.j.rosseinsky@liverpool.ac.uk.
[†] University of Liverpool.
[‡] University of Sydney.

(1) Gardner, G. B.; Venkataraman, D.; Moore, J. S.; Lee, S. *Nature* **1995**, *374*, 792.
(2) Batten, S. R.; Robson, R. *Angew. Chem., Int. Ed.* **1998**, *37*, 1460.
(3) Zaworotko, M. J. *Angew. Chem., Int. Ed.* **2000**, *39*, 3052.
(4) Seo, J. S.; Whang, D.; Lee, H.; Jun, S. I.; Oh, J.; Jeon, Y. J.; Kim, K. *Nature* **2000**, *404*, 982.
(5) Barton, T. J.; Bull, L. M.; Kelmperer, W. G.; Loy, D. A.; McEnaney, B.; Misono, M.; Monson, P. A.; Pez, G.; Scherer, G. W.; Vartuli, J. C.; Yaghi, O. M. *Chem. Mater.* **1999**, *11*, 2633.
(6) Abrahams, B. F.; Hoskins, B. F.; Liu, J. P.; Robson, R. *J. Am. Chem. Soc.* **1991**, *113*, 3045.
(7) Abrahams, B. F.; Hoskins, B. F.; Robson, R. *Chem. Commun.* **1990**, *1*, 60.
(8) Chen, B.; Eddaoudi, M.; Hyde, S. T.; O'Keeffe, M.; Yaghi, O. M. *Science* **2001**, *291*, 1021.
(9) Kuznicki, S. M.; Bell, V. A.; Nair, S.; Hillhouse, H. W.; Jacubinas, R. M.; Braunbarth, C. M.; Toby, B. H.; Tspatsis, M. *Nature* **2001**, *412*, 720.
(10) Noro, S.-i.; Kitagawa, S.; Kondo, M.; Seki, K. *Angew. Chem., Int. Ed.* **2000**, *39*, 2082.
(11) Dyer, A. *An Introduction to Zeolite Molecular Sieves*; John Wiley & Sons: New York, 1988.
(12) Kepert, C. J.; Prior, T. J.; Rosseinsky, M. J. *J. Am. Chem. Soc.* **2000**, *122*, 5158.
(13) Kepert, C. J.; Rosseinsky, M. J. *Chem. Commun.* **1999**, 375.
(14) Li, H.; Eddaoudi, M.; O'Keefe, M.; Yaghi, O. M. *Nature* **1999**, *402*, 276.
(15) Li, H.; Eddaoudi, M.; Groy, T. L.; Yaghi, O. M. *J. Am. Chem. Soc.* **1998**, *120*, 8571.

10.1021/ja0262737 CCC: $22.00

has been described as zeolite-like. However, recent papers have indicated that the behavior of metal-organic framework materials may not be as simple as has been assumed thus far. In the zinc−benzenedicarboxylate system, it was found that the desolvated materials underwent solid-state transformations in response to guest loss,[16] rationalized by comparison of the material with inclusion compounds, where the guest acts as a spacer which supports the host, rather than robust porous materials. In the nickel−bipyridine−ethanol system, a series of guest loading experiments revealed the presence of steps in the type I isotherm which were ascribed to guest-directed structural rearrangement of the host framework material.[17] This is clear evidence that although this material contains porosity, as shown by the overall shape of the adsorption isotherm, it undergoes a structural rearrangement which cannot be understood with reference to zeolites, where the framework structure is largely insensitive to the presence of guests. Other studies on coordination polymer materials have shown hysteresis in the adsorption/desorption isotherms.[18−20] This was ascribed to guest-directed rearrangement of the framework, although the structural cause of this behavior is unclear. The initial low uptake observed in these materials suggests that they cannot be considered microporous.

Here, we present a detailed study of the properties of the porosity found in the methanol-templated phase Ni_2(4,4′-bipyridine)$_3$$(NO_3)_4$ (**A**). 4,4′-Bipyridine (bipy) is a prototypical ligand for the construction of metal-organic frameworks by bridging two metal centers.[21] The possibility of extending the pyridyl linkage[22,23] to produce materials with increased non-framework volume gives access to materials with a wide range of network topologies. The properties of the porosity determined for the Ni−bipy compound currently under investigation are likely to be reproduced to some extent in porous materials in these extended-linkage systems, and the porosity in the Ni−bipy system can therefore be considered as a relatively simple model for the more complex structures which are the state-of-the-art in the area of metal-organic frameworks.

The structures of both the framework and the resulting porosity of **A** have been characterized by single-crystal diffraction from both the methanol-containing as-grown material and the desolvated porous solid, allowing us to identify the limiting dimension in the porosity. This would be expected to lead to guest size selectivity in a rigid microporous solid, and we compare this dimension with the results of sorption experiments. These show that the material possesses a degree of flexibility that is unprecedented in a thermally robust microporous solid, allowing the material to sorb oversized guests. The flexibility of the Ni−bipy system is further demonstrated by the formation of **A** by a guest-driven solid-to-solid transformation from a related microporous crystalline structure.

Experimental Section

Synthetic Method. Phase **A** was prepared by diffusion of $Ni(NO_3)_2$·$6H_2O$ and 4,4′-bipyridyl (bipy) in methanol solution. A 2 mL portion of 0.20 M $Ni(NO_3)_2$·$6H_2O$ (0.1163 g) was placed in one arm of an H-cell (circular cross-section diameter 15 mm, height 90 mm, cross-piece length 60 mm), and a 2 mL portion of 0.20 M 4,4′-bipyridine (0.0624 g) was placed in the other arm. Pure methanol was then carefully layered on top of each solution until the cross piece was full. The cell was then sealed and left undisturbed. Blue rod-shaped crystals of **A** up to 1 mm^3 in volume suitable for single-crystal diffraction experiments were grown over a period of 1 month.

Single-Crystal X-ray Diffraction. Data were collected on a Stoe-IPDS at 193(1) K using Mo Kα radiation ($\lambda = 0.71073$ Å). To minimize any solvent loss from **A**, single crystals were quench-cooled from room temperature by the nitrogen cryostream. Images were recorded for successive rotations of 2° about φ, and the resulting data were reduced using the HKL suite of programs.[24] The structure was solved by direct methods and full matrix least-squares refinements against F^2 for all data using the SHELX97 software package.[25,26] The structural stability of **A** to solvent loss was investigated by characterization of a single crystal of **A** which had been desolvated ex situ at 120 °C. This sample was moved from the desolvating oven to the nitrogen cryostream in ca. 3 min in an attempt to limit the adsorption of atmospheric moisture, and data were recorded at 193(1) K. These data were modeled as described above.

Powder X-ray Diffraction. Powder X-ray diffraction data were collected using a Stoe Stadi-P powder diffractometer in transmission geometry from dried, ground samples contained in 0.3 mm glass capillaries. Use of a curved Ge(111) monochromator allows selection of Cu Kα_1 radiation ($\lambda = 1.54060$ Å). Data were collected using a linear position sensitive detector spanning a 2 Å range of 5.5°, a typical data collection taking 3 h to record the range $7 \leq \Delta 2\theta/\mathrm{deg} \leq 30$ with a step size of $\Delta 2\theta = 0.01°$. In-situ high-temperature X-ray diffraction experiments were carried out using a high-temperature furnace supplied by Stoe & CIE GmbH of Darmstadt, Germany with the sample contained in an open-ended capillary allowing desorbed guests to vent to the atmosphere. The capillary was inserted into the furnace at room temperature, and the temperature was increased up to 170 °C.

Thermogravimetry/Mass Spectroscopy. Thermogravimetric analyses were carried out using a Seiko TG/DTA 6200 thermogravimetry/differential thermal analysis module. Samples were removed from the mother liquor, dried, and ground to a fine powder before placing in a platinum crucible. All TGA experiments were carried out under an atmosphere of He flowing at a rate of 100 mL min^{-1}. Experiments typically used ca. 5 mg of sample and heating rates of 2 °C min^{-1}. The experimental arrangement allowed automatic switching between two gas flows, and this was utilized for the sorption studies by alternating between dry helium and helium saturated with the desired solvent. The outlet gas from the TGA was monitored using a Hiden HPR20 quadrupole mass spectrometer. The quantity of toluene in the gas stream was followed by monitoring mass peaks 65, 91, and 92, and the absence of smaller molecules was confirmed by following mass peaks 29, 31, and 43.

Gas Chromatography. The presence of toluene in the pores of **A** was investigated by gas chromatography. One microliter portions of liquid were injected into an Alltech Econo-Cap EC-1000 column, and the detection was carried out using a Dani 3800 gas chromatograph. The instrument was calibrated using a mixture of toluene (0.04 mL, 0.376 mmol) and 2-ethyl butan-1-ol (0.24 mL, 1.95 mmol) in benzyl alcohol (2.0 mL, 19.45 mmol). An N_2 carrier gas pressure of 60 kPa

(16) Edgar, M.; Mitchell, R.; Slawin, A. M. Z.; Lightfoot, P.; Wright, P. A. *Chem.-Eur. J.* **2001**, *7*, 5168.
(17) Fletcher, A. J.; Cussen, E. J.; Prior, T. J.; Rosseinsky, M. J.; Kepert, C. J.; Thomas, K. M. *J. Am. Chem. Soc.* **2001**, *123*, 10001.
(18) Li, D.; Kaneko, K. *Chem. Phys. Lett.* **2001**, *335*, 50.
(19) Kitaura, R.; Fujimoto, K.; Noro, S.-i.; Kondo, M.; Kitagawa, S. *Angew. Chem., Int. Ed.* **2002**, *41*, 133.
(20) Seki, K. *Phys. Chem. Chem. Phys.* **2002**, *4*, 1968.
(21) Moulton, B.; Zaworotko, M. J. *Chem. Rev.* **2001**, *101*, 1629.
(22) Blake, A. J.; Champness, N. R.; Hubberstey, P.; Li, W.-S.; Withersby, M. A.; Schröder, M. *Coord. Chem. Rev.* **1999**, *183*, 117.
(23) Pschirer, N. G.; Ciurtin, D. M.; Smith, M. D.; Bunz, W. H. F.; zur Loye, H.-C. *Angew. Chem., Int. Ed.* **2002**, *41*, 583.
(24) Otwinowski, Z.; Minor, W. In *Processing of X-ray Diffraction Data Collected in Oscillation Mode*; Otwinowski, Z., Minor, W., Eds.; Academic Press: New York, 1996; p 276.
(25) Sheldrick, G. M. *SHELXS-86*; Universität Gottingen, 1986.
(26) Sheldrick, G. M. *SHELXL-93 Program for the Refinement of Crystal Structures*; Universität Gottingen, 1993.

and a 135 °C isotherm resulted in baseline resolution between toluene and 2-ethyl butan-1-ol (EB). The GC trace showed peaks due to toluene and EB at 1.83 and 2.35 min, respectively, which had a relative ratio of 1:3.8(4) by area. To clear the column after the determination of the toluene:EB ratio, the column was heated to 220 °C for 5 min.

Docking Calculations. Monte Carlo docking calculations were performed with the Solids Docking module of the MSI Insight II software, using the combined valence force field (CVFF) on a Silicon Graphics Indigo2. Allowing the empty framework to relax gave unreasonably short bond distances around the Ni^{2+} centers (observed ca. 2.1 Å vs calculated ca. 1.6 Å), and it was therefore decided to use a rigid framework for the docking calculations. The framework atoms were fixed at the positions determined experimentally using single-crystal X-ray diffraction data from the empty microporous solid. As the calculations were undertaken to provide a description of the steric constraints on the docked guest molecules rather than an estimate of the energy of the docked structures, the absence of a good description of the Ni^{2+} coordination in no way detracts from the validity of the results obtained. Calculations were carried out for docking of methanol and toluene. As both of these molecules have only limited flexibility, they were docked as rigid guests in a two-stage process, in which a Monte Carlo algorithm was initially employed to probe a large number of docking site arrangements, the most successful of which were then subjected to energy minimization. This has been shown to be an effective method of sampling a wide range of different docked structures.[27]

Two calculations were undertaken: the first was to dock two methanol molecules into a single large void, and the second was to dock a single toluene molecule into a unit cell of the framework. For the former, the initial placements and orientation of the first guest molecule were made at random within a limited volume which included a single large void. The interaction energy was then calculated, and the arrangement was rejected if the energy of the bound structure was greater than 2 kcal mol^{-1}. If the energy of the docked arrangement was less than this threshold, the process was repeated for a second guest molecule which was docked into the structure composed of the rigid host and static guest. Again, the arrangement was rejected if the energy was greater than 2 kcal mol^{-1}, and the process was repeated up to a limit of 10 000 iterations. If this iteration limit was reached, the docked structure was eliminated, and the process was recommenced with the docking of the first methanol guest. A total of 10 docked structures was generated by this process. Each of the successfully docked structures was then subjected to an energy minimization in which the conformations of the guest molecules were allowed to vary. The value of the threshold energy used in these calculations was determined by trial and error. The value of 2 kcal mol^{-1} resulted in an accepted structure after an average of 150 300 iterations. Repetition of the entire process resulted in reliable reproduction of the docked structures, demonstrating the efficiency of the technique in probing the possible guest−host arrangements.

Results

Structural Characterization. The reaction of Ni^{2+} and bipy in methanol resulted in the formation of a phase, **A**, which is isostructural with a known material.[28] The structural refinement against single-crystal diffraction data resulted in the fit parameters R1 = 0.0509, wR = 0.1196 (for 752 data with $I > 2\sigma(I)$) and R1 = 0.1203, wR = 0.1390 (for all 1604 data). A total of 133 parameters was refined, and two restraints were employed. **A** contains nickel cations coordinated to three bipy molecules resulting in a "T" shaped linking unit. The pseudo-square pyramidal coordination around the cation is completed by two monodentate nitrate groups resulting in a charge-neutral framework of stoichiometry $Ni_2(C_{10}H_8N_2)_3(NO_3)_4$. These Ni^{2+} centers are linked to give a ladder structure as shown in Figure 1. The bipy molecules composing the infinite chains of the ladders exhibit positional disorder about the C_2 axis of the molecule, which requires splitting of atom positions in the crystallographic model. Both of the noncoordinating oxygen atoms of the nitrate group display large displacement parameters as a manifestation of positional disorder. These oxygen atoms confer stability on the crystal structure by C−H···O hydrogen bonding to the bipyridyl molecules in neighboring ladders at a distance of 2.72(2) Å shown in Figure 1b, resulting in a pseudo close-packed arrangement of ladders shown in Figure 1c. The Ni centers are separated by 11.265(4) and 11.19(1) Å along the sidearms and the rungs of the ladder, respectively. This results in a void which contained significant peaks in the difference Fourier map after the framework atomic parameters had been satisfactorily refined to convergence. Use of the SQUEEZE routine within the PLATON suite of programs[29] gave an estimate of 44.8 electrons per formula unit in the voids which we assign to two disordered methanol molecules, that is, a guest volume of 134.2 $Å^3$.[17] Insertion of oxygen and carbon atoms at the positions indicated by the electron density map did not allow physically sensible nonbonded contacts to the framework. Monte Carlo docking of two methanol guests into a fixed framework was therefore employed to determine if the void space available was capable of accommodating two methanol molecules on steric grounds. This resulted in a docked structure in which all intermolecular distances were greater than 2.2 Å, that is, approximately 90% of the distance expected from van der Waals radii. It is likely that the disorder observed in the single-crystal structure is indicative of local relaxation to better accommodate these molecules.

The purity of the sample was established by powder X-ray diffraction experiments. These data showed good agreement with a powder diffraction pattern calculated on the basis of the structure determined by single-crystal X-ray diffraction. The material readily loses the methanol guest molecules on standing at room temperature for 35 min. TGA and in-situ powder X-ray diffraction demonstrate that **A** is stable up to 215(4) °C; the latter reveals that the maximum lattice parameter change is 1.66(4)% along the *b*-direction on heating to 170 °C, an order of magnitude larger than that observed in *a* and *c* (0.20(5)%). The rigidity of the structure is defined in the *a* and *c* directions by the arms and rungs of the ladders, respectively, while order is maintained in the *b* direction by hydrogen bonding. The hydrogen bonding is more flexible than the covalent bonds which define the *a* and *c* directions, and the anisotropic expansion is a manifestation of this.

X-ray diffraction experiments performed on single crystals which had been heated ex situ to 120 °C in air showed the structure was largely unchanged on desolvation. Structural refinement was carried out using the above structure as a starting model to give final fit parameters R1 = 0.0561, wR = 0.1411 (for 535 data with $I > 2\sigma(I)$) and R1 = 0.1558, wR = 0.1703 (for all 1317 data). A total of 120 parameters was refined, and no restraints were employed. Treatment of the data with the SQUEEZE routine showed a reduction in the cavity population

(27) Freeman, C. M.; Catlow, C. R. A.; Thomas, J. M. *Chem. Phys. Lett.* **1991**, *186*, 137.
(28) Losier, P.; Zaworotko, M. J. *Angew. Chem., Int. Ed. Engl.* **1996**, *35*, 2779.
(29) Spek, A. L. *PLATON, A Multipurpose Crystallographic Tool*; Utrecht University: Utrecht, The Netherlands, 2001.

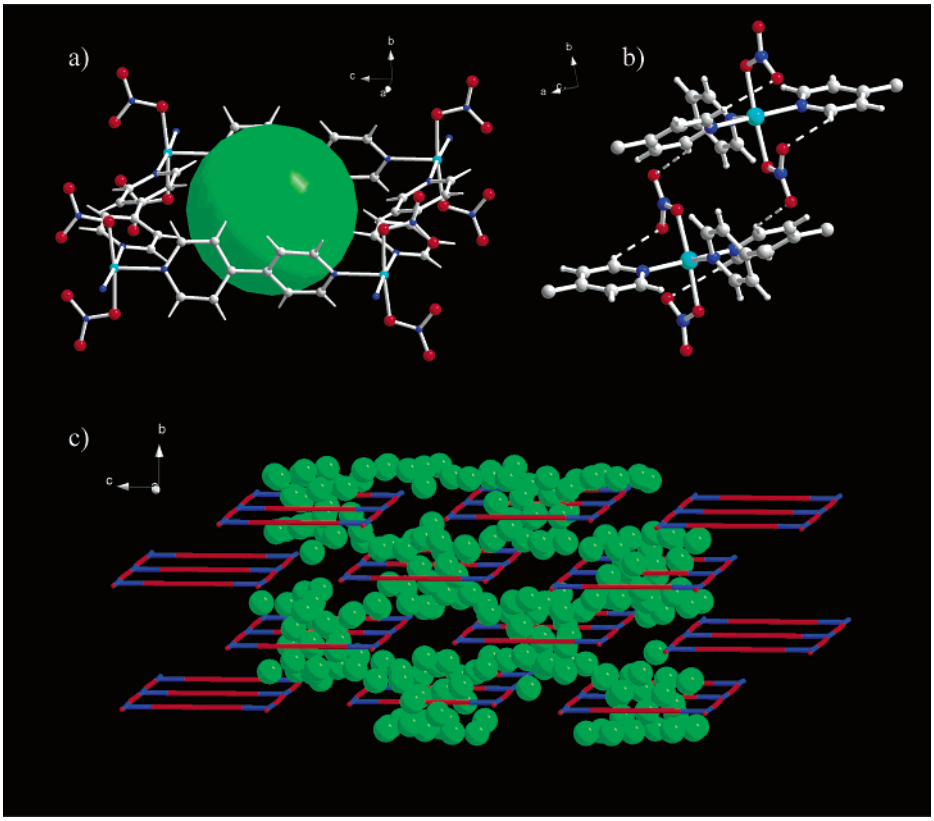

Figure 1. (a) An illustration of the framework surrounding the center of the largest pore. The pore is represented by a green sphere of radius 3.5 Å. The pore surface is composed of the π system of the aromatic rings, the hydrogen atoms of the pyridyl rings, and the noncoordinating oxygen atoms of the nitrate groups. Framework Ni, C, H, N, and O atoms are shown as small cyan, gray, white, blue, and red spheres, respectively. (b) The three-dimensional order is maintained by hydrogen bonds (one per nitrate group) illustrated with dotted lines. Ni, C, H, N, and O atoms are represented by cyan, gray, white, blue, and red spheres, respectively. (c) The pore structure of $Ni_2(4,4'\text{-bipyridine})_3(NO_3)_4$ (**A**). Volume unoccupied by the framework atoms (as determined using ORTEX)[30,31] is indicated by green spheres of 1 Å radius. Only the Ni^{2+} cations (blue) and pyridyl centroids (red) are shown for clarity. In the ladder structure, the Ni centers are separated by 11.27 Å along the sidearms and 11.19 Å by the rungs.

to 17 electrons per formula unit, the nonzero value presumably originating from uptake of atmospheric moisture. On desolvation, **A** undergoes a 0.53(9)% reduction of the *b* lattice parameter, which contributes to a reduction in the unit cell volume of 0.73(10)%. The small magnitude of this contraction means that we cannot assign a cause unambiguously. The Ni coordination environment is unchanged within the precision of the model, and there is no appreciable change in the torsion angles of the bipy molecules.

Sorption Behavior. Thermogravimetric analyses and sorption experiments show that **A** will also take up ethanol to give **A**·$1.1C_2H_5OH$ (a guest volume of 112.2 $Å^3$).[17] Repeated ethanol sorption/desorption shown in Figure 2 demonstrates that this process is reversible, and subsequent X-ray powder diffraction data show that crystallinity is maintained over the six cycles studied.

The large pores shown in Figure 1c are linked by windows which are approximately rectangular in shape, with dimensions defined by the bipyridyl and nitrate groups as shown in Figure 3. The average van der Waals contact distance in the former is 1.8 Å, but disorder allows this to increase up to a maximum value of 2.5 Å, and the maximum window size perpendicular to this direction is 4.9 Å. These distances are predominantly along the *b* and *a* directions of the unit cell, and the observed thermal expansion suggests an increase in window size of only 0.042 and 0.009 Å, respectively, over the range $20 = T/°C = 170$. Therefore, the observed mobility of ethanol (which has a minimum dimension[17] of 4.2 Å) through the porosity is unexpected.

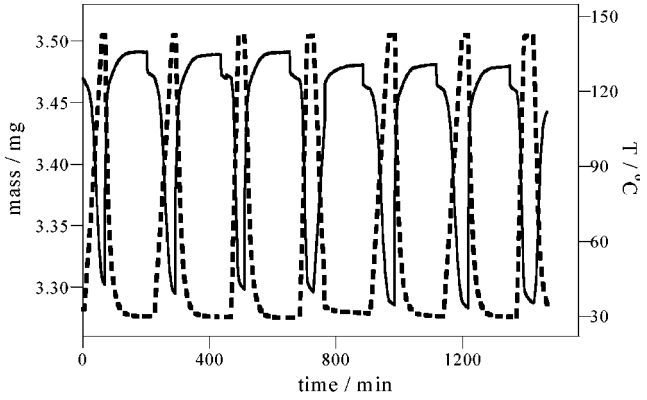

Figure 2. The variation in mass of **A** in response to six cycles of exposure to ethanol vapor at room temperature and heating to 140 °C. The mass (solid line) and temperature (dashed line) as a function of time are shown.

To determine experimentally the effective pore window size, we carried out sorption experiments with the rigid probe molecules toluene and 1,3,5-triethylbenzene. The minimum cross-sectional area of the former is 26.6 $Å^2$ (given by the minimum dimensions 4.012 and 6.625 Å),[32] and this is

(30) Burnett, M. N.; Johnson, C. K. *ORTEP III: Oak Ridge Thermal Ellipsoid Plot Program for Crystal Structure Illustrations, Oak Ridge National Laboratory Report ORNL-6895*; Oak Ridge National Laboratory, 1996.
(31) McArdle, P. *J. Appl. Crystallogr.* **1995**, *28*, 65.

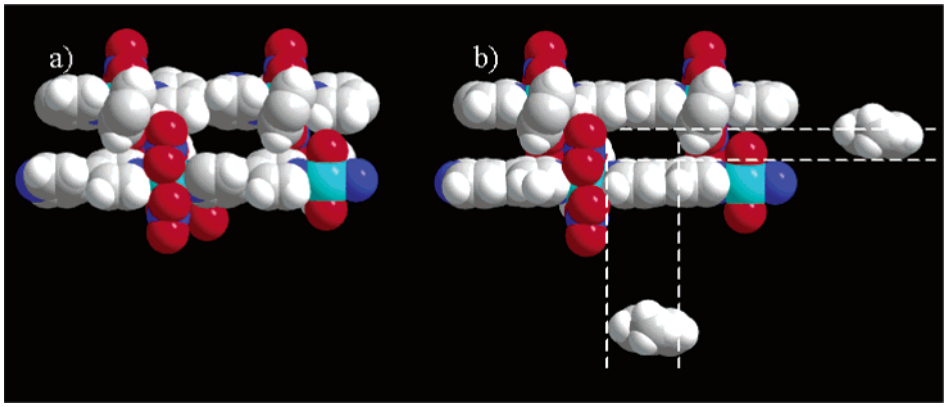

Figure 3. The pore windows of **A**. The dimensions of the windows are defined by bipyridyl molecules and nitrate groups. Ni, C, H, N, and O atoms are represented by cyan, gray, white, blue, and red spheres, respectively. The rocking observed in the bipyridyl molecules allows a range of window sizes; the mean atomic positions are shown in (a), and the maximum window size is shown in (b). The minimum area projected by toluene molecules (shown at the same scale as the framework) indicates that this guest is too large to fit through the windows of **A** determined from the diffraction data.

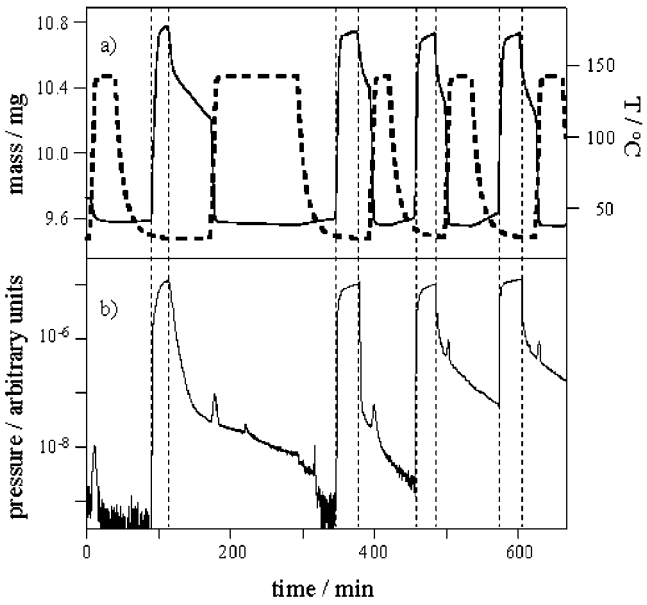

Figure 4. The sorption of toluene by **A**. (a) TGA of the repeated uptake of toluene by **A**. The TGA (a) shows the mass (solid line) and temperature (dashed line) as a function of time. (b) The quantity of toluene in the gas stream as monitored by mass spectrometry of the exit gas, observing the characteristic 91 *m*/*z* peak of the guest (displayed on a logarithmic scale). The simultaneous local maxima in the mass spectrum intensity and mass loss observed upon heating toluene-loaded **A** indicate that both sorption and desorption processes are due to uptake and loss of toluene rather than of adventitious guests. Vertical dashed black lines indicate the switching of the He flow between dry and saturated with toluene vapor.

compared with the pore window size of **A** in Figure 3. The powdered sample was completely desolvated at 140 °C, cooled to room temperature, and exposed to toluene vapor. This resulted in a mass increase, indicating that this guest is accommodated within the porosity of **A** up to a value of 1.20(5) molecules per formula unit (guest volume 212.3 Å^3)[32] in ca. 15 min as demonstrated in Figure 4. The uptake of toluene was confirmed by in-line mass spectrometry.

Postsorption gas chromatography was used to provide an independent check on the presence of toluene in the loaded sample. First, 23.3 mg of **A** was loaded using toluene vapor carried in helium on the TGA. This material was then stored under dry, flowing helium for 10 min to allow any toluene condensed on the surface of the powder to evaporate before being immersed in a mixture of EB (0.0094 mL) and benzyl alcohol (0.1406 mL). GC traces recorded ca. 2 h after the solid had been immersed in the liquid showed the appearance of a peak at 1.83 min which can be assigned unambiguously to toluene. The toluene and EB peaks have relative intensities of 1:4(1), indicating that the mixture contained 1.6(4) μL of toluene. The baseline level observed in the GC trace shows that no other significant components were present in the mixture. This quantity of guest has a mass of 1.4(3) mg, indicating that the observed mass increase is due to toluene uptake. We note that this independent evidence of the presence of toluene was sought after we identified mass increases in other sorption experiments due to the adventitious uptake of impurities in the solvent used.

Powder X-ray diffraction data showed the toluene-loaded material retained the structure of the pristine material with a negligible (0.06%) increase in cell volume (Supporting Information). Monte Carlo docking calculations identified the minimum energy site for the toluene guest to be the center of the large pores, as illustrated in Figure 5, with host−guest nonbonded distances similar to those found in the modeled methanol-loaded structure, demonstrating that the observed loading level is consistent with the essentially undistorted structure of toluene-loaded **A** observed. The similarly sized benzyl alcohol is excluded by **A**, indicating that the framework is selective to specific functional groups. The larger 1,3,5-triethylbenzene (5.3 × 8.2 Å) is not sorbed by **A**, the small mass increase observed (Supporting Information) corresponding to only 0.13(1) molecules per formula unit, assigned to condensation of vapor on the surface of the material.

Transformation Behavior. Synthesis of a Ni−bipy−nitrate framework in ethanol in a manner similar to that described above affords **B**, $Ni_2(bipy)_3(NO_3)_4 \cdot 2C_2H_5OH$.[13,33,34] This material contains a T-shaped coordination around the Ni^{2+} cation similar to that found in **A**, but these T-shaped units are linked together in a different arrangement, resulting in a two-dimensional bilayer structure.[13] **B** is stable to guest loss,[13] and the resulting microporous material readily sorbs methanol. As the ethanol-

(32) Webster, C. E.; Drago, R. S.; Zerner, M. C. *J. Am. Chem. Soc.* **1998**, *120*, 5509.
(33) Kondo, M.; Yoshitomi, T.; Seki, K.; Matsuzaka, H.; Kitagawa, S. *Angew. Chem., Int. Ed. Engl.* **1997**, *36*, 1725.
(34) Power, K. N.; Hennigar, T. L.; Zaworotko, M. J. *New J. Chem.* **1998**, *1998*, 177.

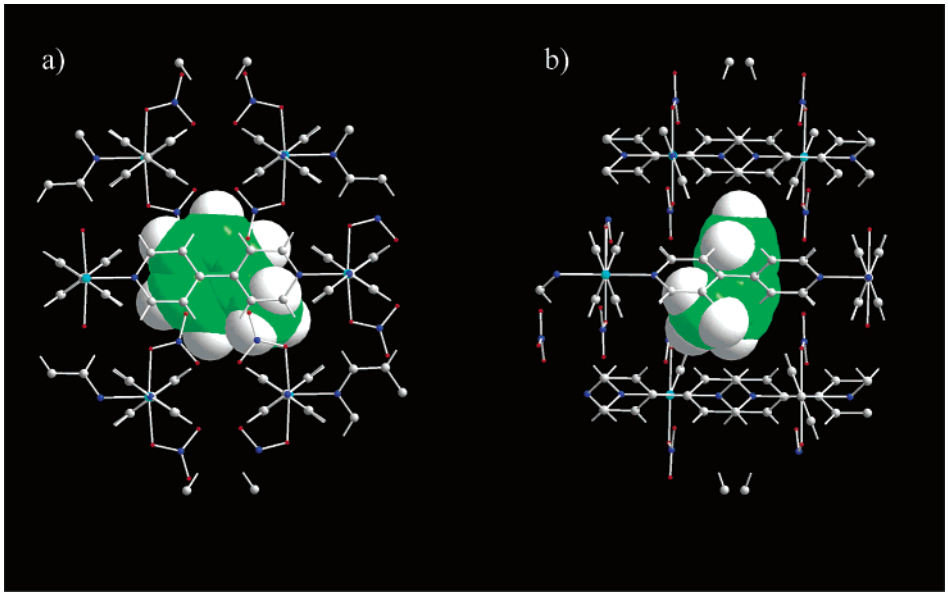

Figure 5. The location of a docked toluene molecule in **A**. The toluene guest in a single large pore determined by Monte Carlo docking calculations after reducing the symmetry of the (fixed) framework to P1 (a) viewed along [100] and (b) along [001]. Only framework atoms which lie within 7 Å of a guest atom are shown. The C and H atoms of the guest molecule are represented by green and white space filling spheres, respectively. The pore surface is composed of the π system of the aromatic rings, the hydrogen atoms of the pyridyl rings, and the noncoordinating oxygen atoms of the nitrate groups. Framework Ni, C, H, N, and O atoms are shown as small cyan, gray, white, blue, and red spheres, respectively.

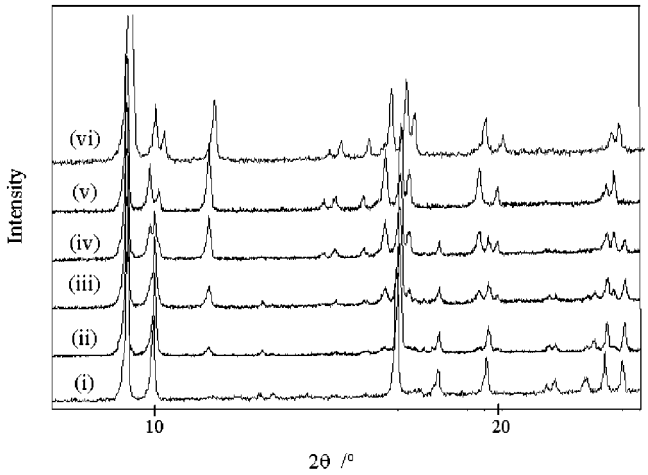

Figure 6. The transformation of **B** to **A** observed by X-ray powder diffraction. X-ray powder diffraction patterns recorded from (i) desolvated ethanol-templated $Ni_2(4,4'\text{-bipyridine})_3(NO_3)_4$ phase **B** after exposure to methanol vapor for (ii) 1 h, (iii) 3 h 40 min, (iv) 7 h 25 min, (v) 22 h 30 min and from (vi) the solvated methanol-templated phase **A**·$2CH_3OH$. Pattern (v) can be fully indexed using a unit cell of dimensions a = 11.263(2) Å, b = 20.569(4) Å, c = 34.395(6) Å, V = 7968.24(1) Å^3.

templated framework structure differs from that grown from a solution of the reagents in methanol, it follows that the sorption of methanol into the ethanol-templated structure results in a metastable phase. Desolvation of the powdered ethanol-templated material **B** at 180 °C for 1 h followed by room-temperature exposure to the static atmosphere above a reservoir of methanol caused a rapid transformation to the methanol-templated structure **A**. Figure 6 shows the X-ray powder diffraction data collected from aliquots removed from the methanol atmosphere as a function of time. These showed that the transformation was underway in the bulk within 1 h and completed within 22 h of the first exposure to methanol. The peak widths of both of the phases showed no evidence of a loss of crystallinity or increased background, showing that this process does not proceed via an amorphous intermediate. The dimensions of the unit cell of the resulting structure are similar to those of as-grown **A**, and the peak widths are identical to those obtained from powdered crystals of the templated material; that is, the crystallinity of the material is not degraded by the transformation. The reaction is quenched by removing the solid from exposure to the methanol source.

Samples of **B** which had been desolvated and fully loaded with methanol and then isolated from methanol vapor remained crystalline and retained the structure of **B** over at least 3 months. Passage of methanol vapor carried in helium over desolvated **B** also failed to effect a transformation over 4 days. Both of these observations indicate that surface-condensed methanol is required for the transformation.

An obvious mechanism for this transformation would involve dissolution of **B** in this methanol followed by crystallization of **A**. To exclude this possibility, we repeated the experiment under conditions which allowed us to observe individual crystals. We repeated the experiment using unground aggregates of crystals of distinctive morphology. These aggregates, up to 0.3 mm in size, were observed under an optical microscope at 60 times magnification and were not moved during the exposure to methanol which was carried out in a dish with a transparent glass lid. The material was thus observed in situ throughout the experiment. After 1 day of exposure, the crystals showed no change in size, external morphology, position, or orientation. Three aggregations of material were removed from the methanol atmosphere, ground, and characterized using X-ray powder diffraction. This showed that the material had undergone the transformation **B** to **A**. There was no evidence of remnant **B** in the sample.

Discussion

Docking calculations, TGA, and X-ray diffraction experiments have shown that the structure of **A** is capable of accommodating toluene within the large cavities in the structure

without any disruption to the framework. However, the minimum cross-sectional area of toluene is double that which can pass through the windows in the porosity which provide access to this cavity. The passage of toluene through the windows would require an expansion of the unit cell that would be clearly manifested in the lattice parameters, but the X-ray diffraction data collected from toluene-loaded material show no change in crystal structure in response to toluene loading. Admission of toluene through the windows must therefore proceed by an expansion of the window size for only as long as is required for the passage of a toluene molecule; the structure then relaxes back to the structure identified by the docking calculations; that is, the framework atoms reside on the positions determined for the as-made material. It is important to recall that the porous framework is thermally stable to 215 °C, demonstrating that the oversized toluene guest is dynamically distorting a structure that is not intrinsically unstable. We have previously shown[17] that **B** shows steps in the sorption isotherms for methanol sorption which were interpreted as modifications of the framework structure in response to guest loading.[17]

Other studies have shown that coordination polymer materials can display a gate effect where initial uptake is negligible but the porosity is "switched on" when a certain pressure is reached. These studies[18−20] do not include structural refinement of the desolvated, porous frameworks, and it is therefore probable that this interesting sorption behavior is related to restoration of porosity to a structure which has undergone relaxation on guest loss. In the present case, single-crystal diffraction experiments have shown that the framework is unchanged on loss of guest.

Whereas the steps or hysteresis observed in these isotherms are symptomatic of a large-scale rearrangement of the framework existing for the duration of the experiment, the observation of toluene passage through **A** shows evidence of a different, more dynamic kind of framework flexibility.

These Ni−bipy framework materials have similarities with both zeolites, due to their permanent microporosity, and with supramolecular architectures,[35] such as the lamellar clay mimics,[36] sustained by hydrogen bonding networks, and it is interesting to compare the properties of **A** with both of these classes of materials. The supramolecular architectures differ profoundly from **A** in that the structures are not stable in the absence of a guest; heating to remove the guest drives collapse to an amorphous apohost. This behavior is fundamentally different from the reversible guest sorption/desorption which **A** demonstrates with no change in structure. Supramolecular architectures thus exhibit the long-range flexibility, but not the stability observed in **A**, which is due to the numerous C−H···O hydrogen bonding interactions between the coordinately bonded ladders. Conversely, zeolites, and related oxide-based materials, show stability to guest loss, due to the strong, three-dimensional Si/Al−O linkages throughout the structure, but the strength of these bonds produces a rigid porosity. Rigid size selectivity allows ETS-4 to discriminate between CH_4 and N_2,[9] while more flexible zeolites (such as RHO[37]) are characterized by effective pore sizes 0.4 Å larger than the crystallographically determined equilibrium values,[11] ascribed to cooperative thermal motion, involving rigid unit modes.[38] Clearly, the flexibility in the window size observed in **A** requires a displacement of the framework atoms from their equilibrium positions that is 4 times larger than that observed in zeolites.

Collapse of a framework must proceed by significant variation in either the distances and/or the angles between the nodes in the structure; that is, framework collapse is synonymous with framework flexibility. The development of metal-organic frameworks has seen the field evolve from materials which collapse in the absence of guest to materials which can form single crystals of unprecedented porosity as a consequence of increasing the rigidity of the frameworks.[8] This advance has been described as a move toward zeolite-like porosity. From our results on sorption experiments, we have to conclude that, at least in the Ni−bipy system, the resultant porosity differs greatly from that observed in zeolites. In the latter, the sorption behavior with respect to a guest of a particular size can be largely inferred from a knowledge of the limiting dimension in the porosity (as determined crystallographically). In **A**, we have shown that this correlation no longer holds and that sorption behavior must be determined experimentally. While the crystalline, microporous framework of **A** is indefinitely stable at room temperature and does not collapse until 215 °C, it displays zeolite-like behavior but combined with flexibility akin to that shown in weakly bound hydrogen bonded networks which readily collapse at room temperature.

This combination of rigidity and flexibility has a further consequence: it allows the guests present in the pores to drive the metal-organic framework directly from one solid-state structure to another. Although the transformation from crystalline **B** to crystalline **A** must initiate at the surface, to achieve complete conversion to **A** while conserving the crystalline nature of both solids, the reaction must be propagated through the remaining solid **B**, that is, a solid−solid conversion in which both **B** and **A** are highly crystalline. Although the two structures are similar (e.g., a volume difference of $<1\%$), the structural rearrangement within the solid requires considerable rearrangement of the bipy linking molecules forming the ladders in **A** and the bilayers in **B**, with the breaking of at least one of every six Ni−bipy bonds and subsequent rotation of the bipy unit. The X-ray data indicate that these steps occur without loss of crystallinity, and we have identified two possible mechanisms for the transformation. To transform **B** to **A** with a minimum of bond breaking, it is necessary to break one in six of the Ni−N bonds and proceed via a cooperative volume change as illustrated as steps i and ii in Figure 7. This would be expected to lead to considerable strain in the solid which is not compatible with the results of our X-ray powder diffraction data. Therefore, we favor an alternative mechanism which requires breaking of one in three Ni−N bonds and could occur through a local, noncooperative path shown in Figure 7iii−v. This route would allow the transformation to proceed via the formation of defects of the ladder structure of **A** within a matrix of the bilayer structure of **B**.

Solid-state transformations at room temperature in crystalline materials remain an uncommon occurrence; the chemical bonds which are required to maintain order in the solid usually preclude such behavior. The scale of molecular reorientation required to effect transformation from **B** to **A** is unprecedented in a crystalline transformation. Previous examples have involved

(35) Desiraju, G. R. *Angew. Chem., Int. Ed. Engl.* **1995**, *34*, 2311.
(36) Biradha, K.; Dennis, D.; MacKinnon, V. A.; Sharma, C. V. K.; Zaworotko, M. J. *J. Am. Chem. Soc.* **1998**, *120*, 11894.
(37) Baur, W. H. *J. Solid State Chem.* **1992**, *97*, 243.
(38) Hammonds, K. D.; Heine, V.; Dove, M. T. *J. Phys. Chem. B* **1998**, *102*, 1759.

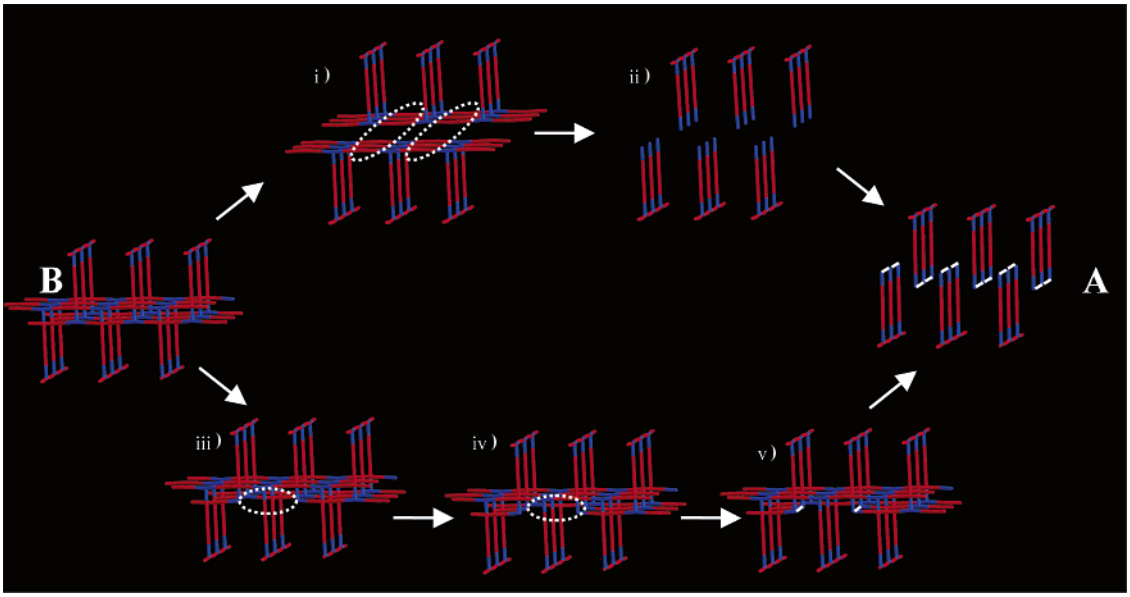

Figure 7. Schematic representation of the structural rearrangement required for transformation from ethanol-templated **B** to methanol-templated **A**. The transformation can proceed by (i) a cooperative expansion followed by (ii) breaking one in three of the Ni−N bonds followed by Ni−N bond formation and contraction to give **A**. Alternatively, the structure of **B** can be transformed by (iii) breaking both Ni−N bonds securing a bipy molecule (circled), (iv) breaking both bonds which secure a parallel bipy (circled), and translating both molecules and bonding to Ni^{2+} cations (v) to give a ladder defect of **A** in a crystal structure otherwise composed of layered **B**. Repeating this process leads to the formation of structure **A**. Structures are depicted as in Figure 1c, and transformed bipy molecules are shown in white.

small molecular rearrangements with minimal disturbance to the crystal structure, such as insertion of SO_2 into an organoplatinum complex,[39] insertion of molecular oxygen into a Sb−Sb bond,[40] coordination changes in an Ag−polynitrile network,[41] or the cyclization of anilide.[42] A more substantial transformation has been observed in response to chloroform exposure between cadmium cyanide framework materials which involved a considerable change in network connectivity.[43] However, the starting material readily decomposes when removed from the mother liquor indicating that the framework is not structurally robust. The framework should therefore be considered to be supported by the solvent occupying the nonframework volume, and it is not surprising that the framework can be disrupted by a change of guest solvent. It has recently been shown that bipyridyl-based frameworks can undergo conversion when immersed in solution containing a different anion for several days.[44] The authors did not report X-ray diffraction data from the partially converted product, and it is probable that the transformation was achieved through dissolution and recrystallization. The considerable and direct guest-driven solid-state transformation between two microporous extended structures observed here is a second demonstration of the differences between the microporous metal-organic frameworks and inorganic oxide framework structures. The transformation and sorption behavior of these materials are linked by a common observation that although the material is structurally stable in the absence of guest and, hence, is porous, the framework is either dynamically or statically unstable when exposed to specific chemical species; toluene modifies the effective window size allowing admittance to the pores within, and ethanol guests can drive the framework to a different structure. This observation leads us to the conclusion that although a metal-organic framework may be demonstrably thermally robust and microporous (as shown by TGA, diffraction experiments, and type I isotherms), it may not be chemically stable in the presence of species which may be otherwise considered innocuous.

Conclusions

We have shown that porous metal-organic frameworks can differ from their classical oxide counterparts through their enhanced flexibility; in the presence of a guest, the pore windows of the thermally robust **A** open to twice their area at rest to allow sorption, and the guests can direct solid-to-solid transformations between porous structures. We note that previous examples of such transformations are not porous phases and therefore cannot be guest-driven locally in the way that we have shown. Considered individually, these phenomena are unprecedented; taken together, they represent the first example of nonzeolitic behavior by a robust microporous metal-organic framework.

Acknowledgment. We are grateful to J. F. Bickley and A. Steiner for experimental assistance and useful discussions and to EPSRC under GR/N08537 for funding.

Supporting Information Available: Figures S1−S9 contain the results of Monte Carlo docking calculations, X-ray powder diffraction data, TGA data, variable temperature X-ray powder diffraction data, mass change on exposure of **A** to variety of vapors (1,3,5-triethylbenzene, benzyl alcohol, and 2-ethyl butan-1-ol), gas chromatography of toluene-loaded **A**, and the rate of conversion of **B** to **A** (PDF). Crystallographic information files are available for as-made **A** and desolvated **A**. This material is available free of charge via the Internet at http://pubs.acs.org.

JA0262737

(39) Albrecht, M.; Lutz, M.; Spek, A. L.; van Koten, G. *Nature* **2000**, *406*, 970.
(40) Tokitoh, N.; Arai, Y.; Sasamori, T.; Okazaki, R.; Nagase, S.; Uekusa, H.; Ohashi, Y. *J. Am. Chem. Soc.* **1998**, *120*, 433.
(41) Min, K. S.; Suh, M. P. *J. Am. Chem. Soc.* **2000**, *122*, 6834.
(42) Hosomi, H.; Ohba, S.; Tanaka, K.; Toda, F. *J. Am. Chem. Soc.* **2000**, *122*, 1818.
(43) Abrahams, B. F.; Hardie, M. J.; Hoskins, B. F.; Robson, R.; Williams, G. A. *J. Am. Chem. Soc.* **1992**, *114*, 10641.
(44) Noro, S.-i.; Kitaura, R.; Kondo, M.; Kitagawa, S.; Ishii, T.; Matsuzaka, H.; Yamashita, M. *J. Am. Chem. Soc.* **2002**, *124*, 2568.